Monte Carlo Simulation of Magnesium Ion in 18.45 mol% Aqueous Ammonia Solution

Suchada Kheawsrikul [a], Supot V. Hannongbua [b], and Bernd M. Rode [a, c]

[a] Department of Chemistry, Faculty of Science, Prince of Songkla University, Hat-Yai, Songkla 90112, Thailand
[b] Department of Chemistry, Faculty of Science, Chulalongkorn University, Bangkok 10330, Thailand
[c] Department of Chemistry, Faculty of Science, University of Innsbruck, A-6020 Innsbruck, Austria

Z. Naturforsch. **46a**, 111–116 (1991); received May 22, 1990

Dedicated to Dr. K. Heinzinger on the occasion of the 60th birthday

A Monte Carlo simulation has been performed for a magnesium ion in 18.45 mol% aqueous ammonia solution at 20 °C, using additive pairwise potential functions obtained from ab-initio calculations. The structural arrangement of the solvent molecules in the vicinity of the ion is discussed in terms of radial distribution functions and average molecular orientations. It was found that the first solvation shell of the ion consists of four water and three ammonia molecules, and the second shell of nine water and five ammonia molecules.

Introduction

Computer simulations can help to find out the structure of solvents surrounding solvated ions [1–5]. Previously the structure of solvated lithium and sodium ions in aqueous ammonia has been reported [6, 7]. It seemed interesting to compare the solvation in this solvent of ions of similar size but different charge, such as Li^+ and Mg^{2+} (ionic radii 0.60 and 0.65 Å, respectively).

In this paper the solvation of magnesium ion in 18.45 mol% aqueous ammonia is evaluated under the same conditions as in the study for Li^+ [6].

Details of the Simulation

The simulation has been performed for a very dilute solution of magnesium ion in 18.45 mol% aqueous ammonia, i.e., the periodic cube contained one magnesium ion, 37 ammonia and 164 water molecules. The experimental density of a 18.45 mol% aqueous ammonia solution, at 20 °C and 1 atm, of 0.9307 $g \cdot cm^{-3}$ has been used, resulting in the side length 18.65 Å of the periodic box. Half of this length was chosen as spherical cut-off. All molecules were assumed to be rigid. The Metropolis sampling algorithm [8] was used. The MCY potential [9] and the H15H potential [10] were employed to evaluate the water/water and ammonia/ammonia interactions, respectively. The TR ammonia/water potential [11], the DRH magnesium ion/water potential [12] and the HKP magnesium ion/ammonia potential [13] were used for the remaining intermolecular interactions.

The starting configuration of the solvent was derived from the simulation of lithium ion in 18.45 mol% aqueous ammonia solution of our previous work [6]. In order to ensure that equilibrium was reached, the temperature was raised to 120 °C after 6.0×10^5 configurations and then lowered again to 20 °C. Starting after the first 10^6 configurations, a further 10^6 configurations were used to evaluate the structural data.

Results and Discussions

a) Radial Distribution Functions

The RDFs, $g_{xy}(r)$, are shown in Figs. 1–3, describing the Mg^{2+}/H_2O, Mg^{2+}/NH_3, H_2O/H_2O, NH_3/NH_3, NH_3/H_2O and H_2O/NH_3 distributions. Also the running integration numbers are shown, which are defined as

$$n_{xy}(r) = 4\pi\varrho \int_0^{r_m} g_{xy}(r)\, r^2\, dr,$$

Reprint requests to Prof. Dr. B. M. Rode, Department of Chemistry, Faculty of Science, University of Innsbruck, A-6020 Innsbruck, Austria.

0932-0784 / 91 / 0100-0111 $ 01.30/0. – Please order a reprint rather than making your own copy.

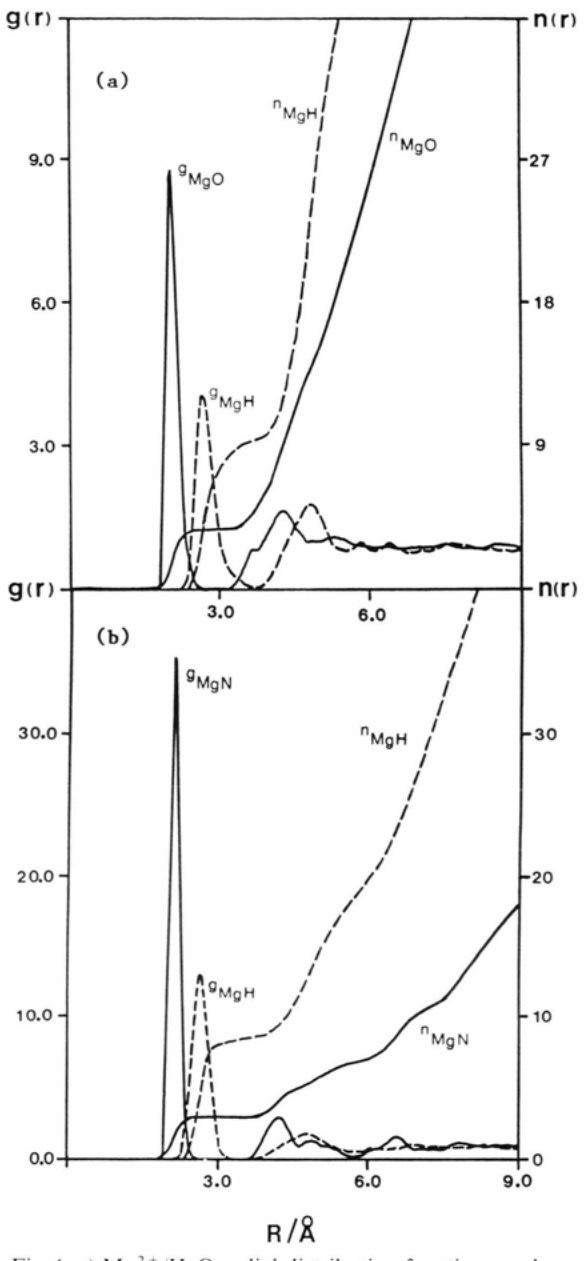

Fig. 1. a) Mg^{2+}/H_2O radial distribution functions and running integration numbers, b) Mg^{2+}/NH_3 radial distribution functions and running integration numbers.

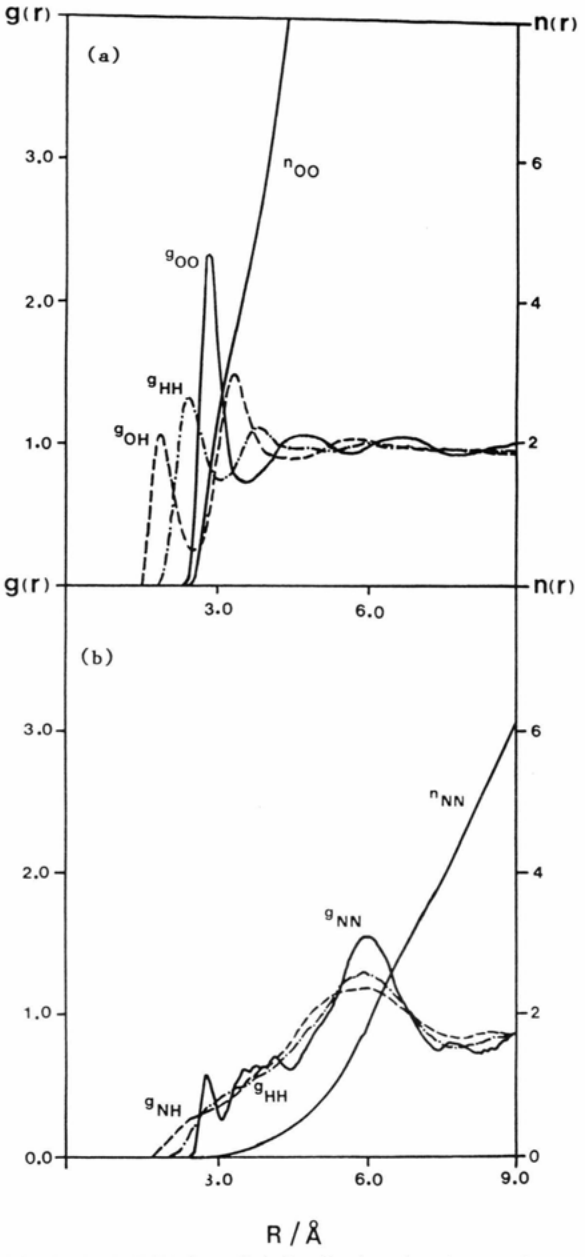

Fig. 2. a) H_2O/H_2O radial distribution functions and running integration numbers, b) NH_3/NH_3 radial distribution functions and running integration numbers.

where ϱ is the number density of the molecules. Characteristic data for RDFs and solvation numbers $n_{xy}(r)$ are given in Table 1.

The corresponding integration numbers are shown. The first peak in $g_{MgO}(r)$ at 2.05 Å is about 0.05 Å farther away than for Mg^{2+} in pure water [12]. The first hydration shell is very well separated from the second one, the number of water molecules in it being rather exactly 4. No exchange of any water molecule between the first and second hydration shell was observed in this simulation, as expected for such strong ion solvent interactions. The region from about 3.2 Å

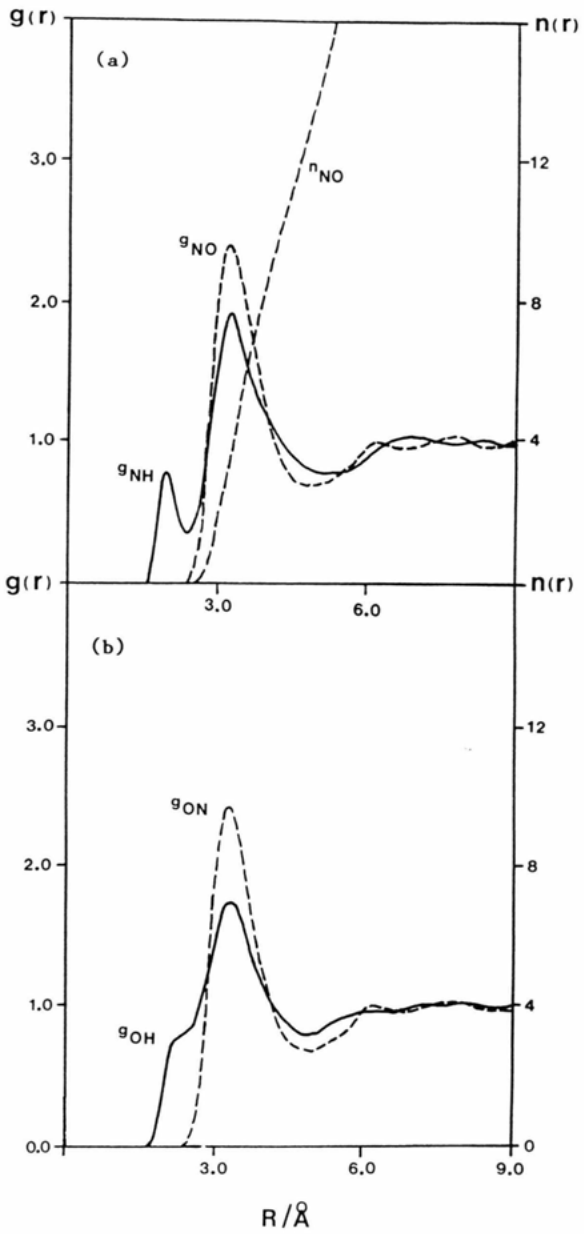

Fig. 3. a) NH_3/H_2O radial distribution functions and running integration numbers, b) H_2O/NH_3 radial distribution functions.

Table 1. Characteristic values of the radial distribution functions for magnesium ion in 18.45 mol% aqueous ammonia solution.

$$n_2 = 4\pi\varrho \int_{1\text{st Min.}}^{2\text{nd Min.}} g(r)\, r^2\, \mathrm{d}r.$$

	1st Max./Å	1st Min./Å	n_1	2nd Max./Å	2nd Min./Å	n_2
Mg(II)–H_2O						
Mg(II)–O	2.05	3.00	4.0	4.30	4.75	9.0
Mg(II)–H	2.70	3.75	8.1	4.90	5.40	34.0
Mg(II)–NH_3						
Mg(II)–N	2.15	2.65	2.8	4.25	4.65	5.0
Mg(II)–H	2.70	3.25	8.5	4.80	5.70	18.0
H_2O–H_2O						
O–O	2.85	3.60	4.2	–	–	–
O–H	1.90	2.55	1.6	–	–	–
NH_3–NH_3						
N–N	2.80	3.05	0.2	–	–	–
NH_3–H_2O						
N–O	3.25	4.80	12.8	–	–	–
N–H	2.00	2.40	1.0	–	–	–
H_2O–NH_3						
O–H	3.25	4.80	12.9	–	–	–
O–H	2.30	2.65	0.7	–	–	–

up to about 4.75 Å corresponds to the second hydration shell with the maximum of the RDF at 4.30 Å and the number of water molecules of ~9. The Mg^{2+}–H RDF shows a well pronounced peak at 2.70 Å. The average coordination number for hydrogen atoms is 8.1, corresponding to the 4 water molecules in the first shell within 3.75 Å. The further RDF region, corresponding to the second hydration shell, is also well resolved in $g_{MgH}(r)$.

The Mg^{2+}–N RDF shows a peak at 2.15 Å, leading to the coordination number of 3.0 up to the minimum at 2.65 Å. This first peak is very sharp, symmetric and well separated from the second layer, quite in contrast to the result for Li^+ [6]. The first Mg^{2+}–H peak appears at 2.70 Å, compared to 3.15 Å for Li^+. These differences reflect the stronger interaction of NH_3 with the divalent ion.

The $g_{OO}(r)$ curve has its first maximum at 2.85 Å, identical to the simulations of pure water [14] and Li^+ in aqueous ammonia [6]. Also $g_{OH}(r)$ and $g_{HH}(r)$ have their first peaks located at positions very similar to those of pure water and Li^+ solution.

The first peak of the N–N RDF is located at 2.80 Å, and integration up to 3.05 Å yields 0.2 ammonia molecules. This small peak was not observed in the Li^+ solution. A second, quite diffuse peak appears at about 4.2 Å, yielding 1 ammonia molecule. The N–H and corresponding H–H functions are flat and broad; hydrogen-bonded ammonia dimers, as existing in

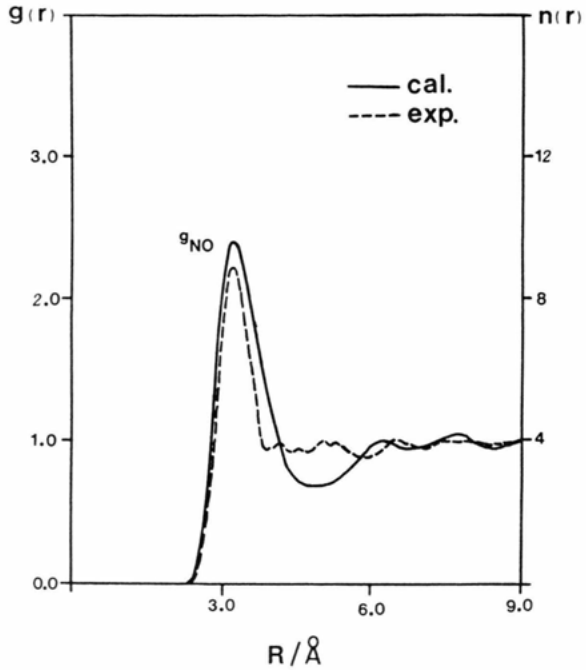

Fig. 4. Comparison of N–O radial distribution functions of the $Mg^{2+}/NH_3/H_2O$ simulation with X-ray scattering data for aqueous ammonia.

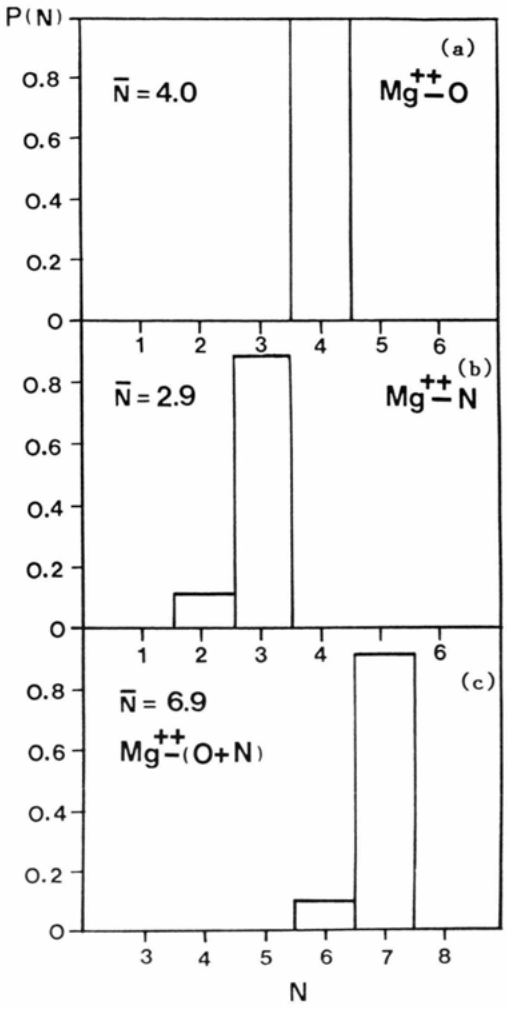

Fig. 5. Distribution of integer coordination numbers for water, ammonia and total solvent molecules in the first shell of magnesium ion.

pure ammonia [15], cannot be recognized in the present system since the N–H(NH_3) RDF is almost structureless.

The N–O RDF shows the first maximum at 3.25 Å, similar to the pure aqueous ammonia solution. The running integration number up to first minimum (4.80 Å) indicates that there are 12.8 water molecules. The contribution of hydrogen bonded configurations can be recognized by the shoulder peak in the N–H(H_2O) RDF around 2.0 Å (Fig. 3a) with 1.0 hydrogen atom compared to 12.8 nearest-neighbour water molecules present. This reveals a rather disturbed solvent structure around ammonia molecules in comparison to the pure aqueous ammonia solution.

The O···H(NH_3) hydrogen bonding is represented by the shoulder peak in the O–H(NH_3) RDF at 2.3 Å (Fig. 3b), an average integration number of 0.7 hydrogen atoms being obtained. This result agrees with the data from the Na^+-NH_3/H_2O [7] and Li^+-NH_3/H_2O [6] simulations.

Figure 4 shows the N–O RDF of this simulation compared to Narten's X-ray scattering data for pure aqueous ammonia [16]. The first peak is located at exactly the same distance. However, at distances above 4 Å, some differences are observed concerning the location of the second and third peak. This, and the cut-off radius employed, let the data for a second solvation shell appear ambiguous, whereas the first shell data should be reliable. The observed differences could, however, also be real, caused by the influence of the doubly charged ion on the solvent structure.

Distribution of Integer Coordination Numbers

For the coordination number analysis, the "first shell cut-off" was chosen at the first minimum of the RDFs. Figure 5 shows the distribution of integer numbers of water, ammonia and total solvent mole-

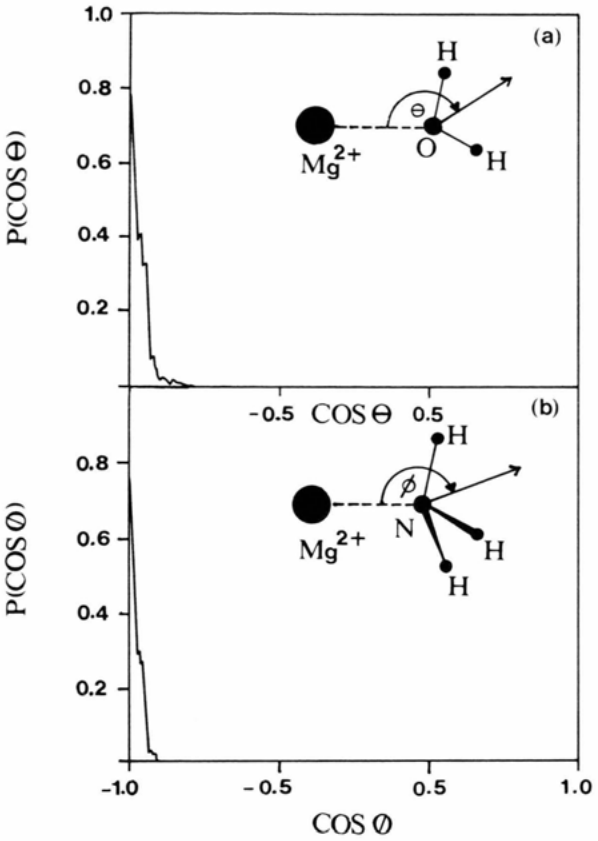

Fig. 6. a) Distribution of orientation of water molecules in the first solvation sphere of magnesium ion and b) distribution of orientation of ammonium molecules in the first solvation sphere of magnesium ion.

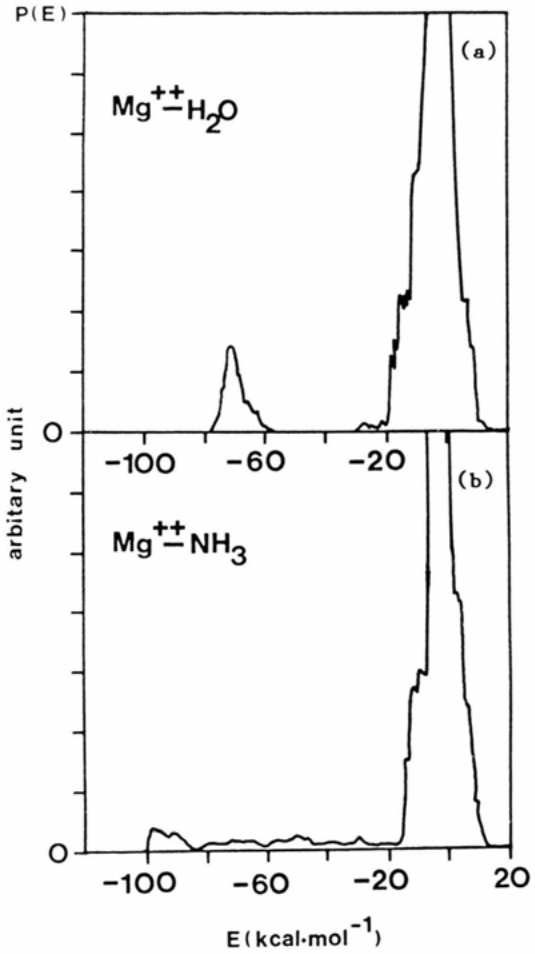

Fig. 7. a) Pair energy distribution of Mg^{2+}/H_2O and b) pair energy distribution of Mg^{2+}/NH_3.

cules in the first shell of Mg^{2+}. Whereas almost exclusively 4 water molecules are in the first shell more variation is observed for the ammonia molecules. These distributions indicate that exchange processes with this shell should dominantly involve ammonia molecules.

Orientation of the Solvent Molecules

Additional information on the structure of the solvated Mg^{2+} is provided by the orientation of solvent molecles in the solvation shells. The orientation of water and ammonium molecules with respect to the ion can be described by the angles θ and ϕ between the dipole moment vectors and the vectors pointing from oxygen and nitrogen to the ion (cf. Figure 6).

In the first solvation shell of Mg^{2+} an extremely sharp distribution maximum is found at $\theta = 180°$, indicating the favourable ion-binding configuration along the C_2 axis of water towards the oxygen's lone pairs. This is similar to the case of water molecules around Na^+ and Li^+ in this solution. Also ammonia molecules are clearly dipole oriented, their distribution displays a sharp maximum at $\phi = 180°$. Similar results were found for Na^+ [7], but not for Li^+, where the ammonia orientation deviates from the dipole orientation by 24°, thus demonstrating the increased structure forming ability of the double charge of an ion with comparable radius.

Distribution of Interaction Energy

The distribution for the interaction energies for water and ammonia molecules bound to the ion is

shown in Figure 7. The highest probabilities, corresponding to interactions with the bulk solvent, are found at -13.5 and -11.2 kcal · mol^{-1} for Mg^{2+}/H_2O and Mg^{2+}/NH_3 interactions, respectively.

For both interactions, further maxima are found, indicating the strong ion-4 H_2O and ion-3 NH_3 interactions in the first shell. The curve for Mg^{2+}/H_2O shows this peak isolated and centered at -70.0 kcal · mol^{-1}. In the case of Mg^{2+}/NH_3, the maximum extends over the region -85 to -100 kcal · mol^{-1}, and there is a non-zero probability virtually over the whole region. This once more indicates the possibility of a continuous exchange of NH_3 molecules between the 1st and 2nd layers. For Li^+/H_2O and Li^+/NH_3, both separations of the first solvation shell are less pronounced. A comparison of the general features of the peaks corresponding to the first shells for Li^+, Na^+ and Mg^{2+} shows that they become smaller and broader with increasing ion size and smaller charge, consistent with electrostatic considerations.

Acknowledgement

Generous supply of computer time by the Computer Center of Prince of Songkla University and the Computer Center of Chulalongkorn University is gratefully acknowledged.

[1] G. Alagona, C. Ghio, and P. A. Kollman, J. Amer. Chem. Soc. **107,** 2229 (1985).
[2] H. Narusawa and K. Nakanishi, J. Chem. Phys. **73,** 4066 (1980).
[3] P. Bopp, I. Okada, H. Ohtaki, and K. Heinzinger, Z. Naturforsch. **40a,** 116 (1985).
[4] G. Palinkas and K. Heinzinger, Chem. Phys. Lett. **126,** 251 (1986).
[5] M. Migliore, S. L. Fornili, E. Spohr, G. Palinkas, and K. Heinzinger, Z. Naturforsch. **41a,** 826 (1986).
[6] S. Kheawsrikul, S. V. Hannongbua, S. U. Kokpol, and B. M. Rode, J. Chem. Soc., Faraday Trans, **2,** 85, 643 (1988).
[7] B. M. Rode and Y. Tanabe, J. Chem. Soc., Faraday Trans. **2,** 1779 (1988).
[8] N. Metropolis, A. W. Rosenbluth, M. N. Rosenbluth, A. H. Teller, and E. Teller, J. Chem. Phys. **21,** 1087 (1953).
[9] O. Matsuoka, E. Clementi, and M. Yoshimine, J. Chem. Phys. **64,** 1351 (1976).
[10] S. V. Hannongbua, T. Ishida, E. Spohr, and K. Heinzinger, Z. Naturforsch. **43a,** 572 (1988).
[11] Y. Tanabe and B. M. Rode, J. Chem. Soc., Faraday Trans. **2,** 84, 679 (1988).
[12] W. Dietz, W. O. Riede, and K. Heinzinger, Z. Naturforsch. **37a,** 1038 (1982).
[13] S. V. Hannongbua, S. Kheawsrikul, and M. M. Probst, J. Sci. Soc., Thailand **15,** 203 (1989).
[14] S. Swaminathan, S. W. Harrison, and D. L. Beveridge, J. Amer. Chem. Soc. **100,** 5705 (1977).
[15] I. R. McDonald and M. L. Kline, J. Chem. Phys. **64,** 4790 (1976).
[16] A. H. Narten, J. Chem. Phys. **49,** 1692 (1968).
[17] S. V. Hannongbua, Kheawsrikul, S. Kokpol, S. Polman, and B. M. Rode, Z. Naturforsch. **42a,** 143 (1988).